The British International School, Shanghai.

Extended Essay

Effects of the Dimensions of a Paper Sheet on its Dart Paper Airplane Product.

Word Count: 3511

Henri Gernaey
2010-2012

Abstract:

The paper dart is one of the simplest and most popular paper airplane models. Although usually made from an A4 sheet of paper, its design varies as the length-to-width ratio of the sheet of paper used to construct it changes, hence also affecting the aerodynamic properties of the airplane. This essay presents the changes in the paper dart design engendered by variations in the dimensions of the paper sheet by considering a range of different length-to-width ratios, and attempts to determine the ratio which produces the best paper dart. Wind tunnel testing was carried out to measure lift and drag forces in order to derive the lift coefficients, drag coefficients, the aerodynamic efficiency and the gliding ability of the darts. Although an A4 format sheet of paper has a length-to-width ratio of 1 : 0.7, it was found and concluded that a paper sheet of length to width ratio 1 : 0.9 produced the most efficient dart. From the data, a theory explaining the different aerodynamic efficiencies of the darts was suggested, proposing that the slight changes in wing profile and that the formation of additional winglets caused by increases in length-to-width ratios were the cause of the efficiency variations. Factors which may arise in practical but which were not considered for the investigation were discussed, and an evaluation of the work containing suggestions for follow up research project was made.

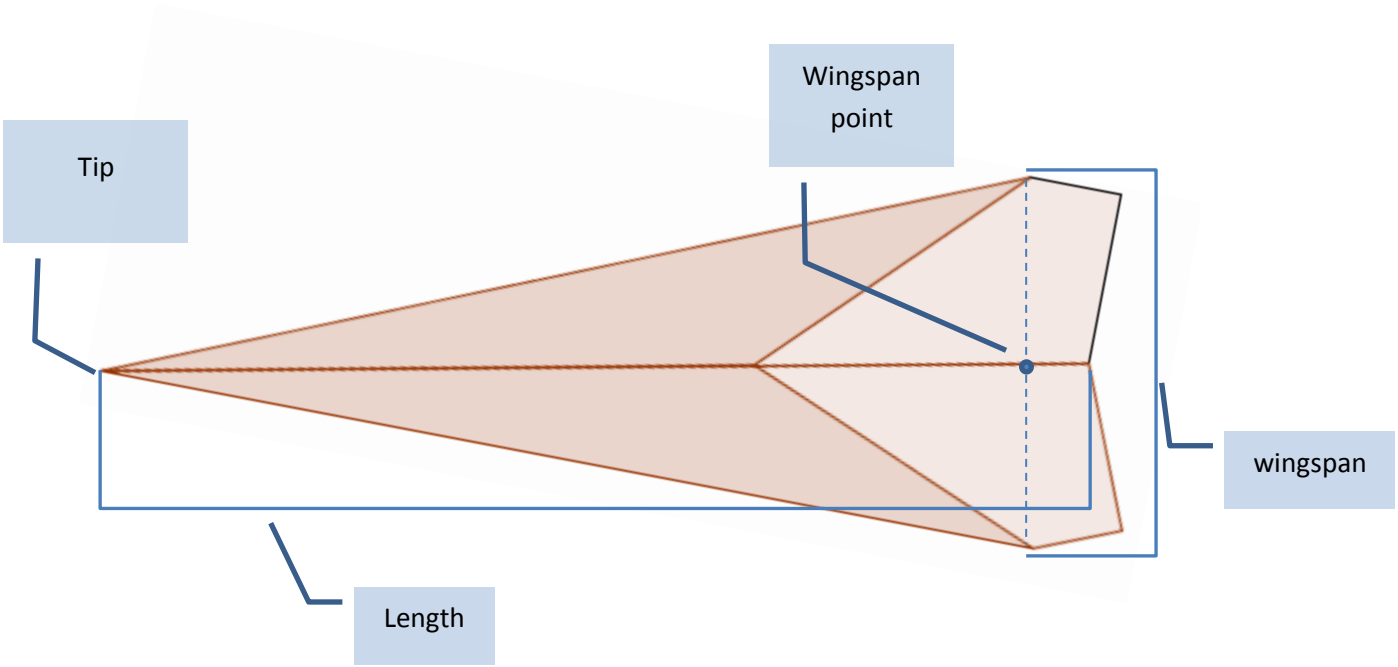

Figure 1 : Anatomy of a paper airplane

Table of Contents

I. Introduction

Paper airplanes trigger curiosity and amazement in all. Although they may often be considered as a juvenile occupation, these seemingly simple structures are subject to all the laws of subsonic aerodynamics, and share characteristics with some of the peaks of technology in the field of aeronautics. Their structural ressemblance to modern aircraft, as well as their low Reynolds-number range similar to that of Micro Air Vehicles (MAV) [1] makes their relevance in the field of aeronautics quite significant. Years of research and trial and error experimenting have been spent in search of the best designs in terms of flight duration and covered distance. To achieve this, the wings must generate the most lift force while producing the smallest drag force as possible to allow the plane to glide on the smallest gradient slope possible, hence flying further and longer. The amount of lift and drag force generated by a wing is proportional to the planform area of the wing (the area of the wing as viewed from above the wing[2]), the density of air and the square of the relative velocity of the wing. The lift and drag force also both depend on a dimensionless quantity called the lift coefficient and drag coefficient respectively. These coefficients differ for every different angle of attack and every different wing profile. Because they are a measure of the *ability* of wing to generate lift or drag, regardless of the other quantities such as the planform area, the lift and drag coefficients are a good way to compare the aerodynamic efficiency of a design in purely structural, not practical, terms.

The aerodynamic efficiency of a wing can be defined as the ratio between the lift coefficient and drag coefficient [3]. The aerodynamic efficiency of a wing can be displayed graphically by plotting the Lift coefficient against the drag coefficient of that wing at different angles of attack (figure 2), generating a relationship called the drag polar curve.

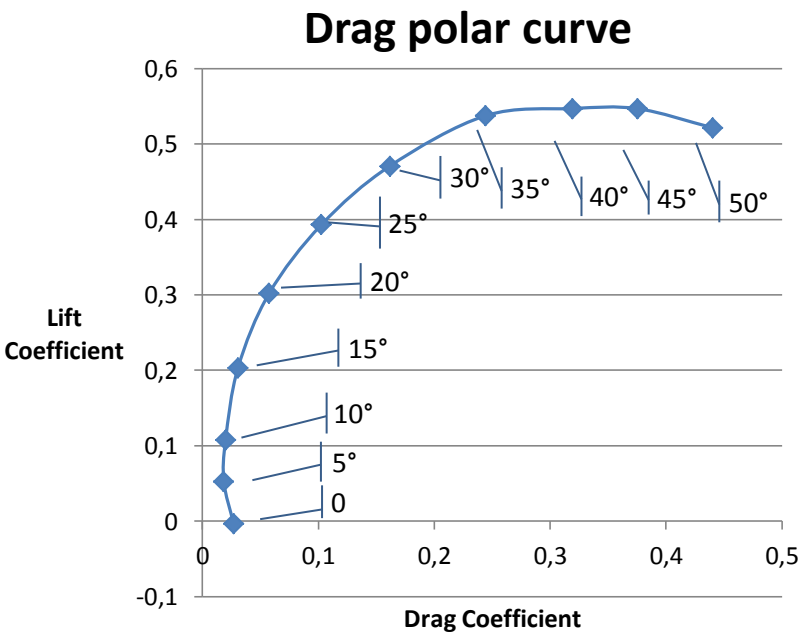

Figure 2 : Example of a drag polar curve

The resulting design of a paper airplane is not only dependent on the folding procedure, but also on the length to width ratio of the starting piece of paper. If the exact same folding procedure is followed, changing this ratio has for effect to cause some variations in the model, and consequently a change in aerodynamic properties. Therefore, it is likely that, for every different paper airplane model, an optimal starting length-to-width ratio would produce a more efficient airplane.

The paper dart is one of the simplest and most popular paper airplane models. Although generally made from an A4 sheet of paper (probably due to the high availability of this format in our society), the dart model could potentially have a higher aerodynamic efficiency if the length-to-width ratio were changed, and the aim of this investigation is therefore to determine the optimal dimensions required to produce the most efficient paper dart.

In order to understand the implications of changing the starting sheet's dimensions, it is important to visualize the anatomy of a common paper dart. Consider an unfolded standard paper dart constituted of an A4 format sheet of paper, as shown in figure 3.

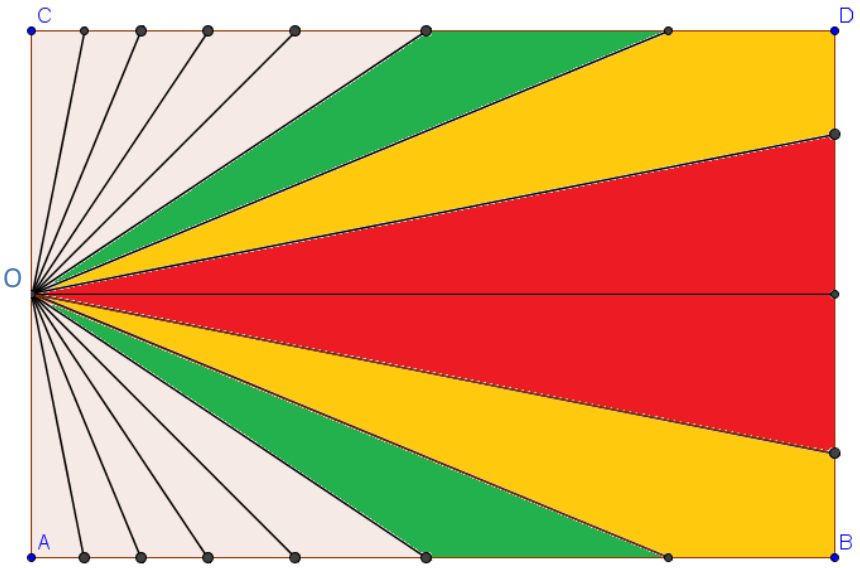

Figure 3 : Unfolded A4 paper dart

The paper dart fold lines being symetrical and all starting from the tip of the airplane cause the angle $\widehat{AOC}$ to be bisected in 16 equal angles of 11.25°. The two orange areas represent the interior faces of the plane's wings, whereas the green areas represent the superior face of the wing, which, when folded, would result in the paper airplane below:

Figure 4 : Upper and side view of a regular A4 paper dart

As the width of the paper sheet changes but the length remains constant (20 cm in table 1), a clear variation in the design of the airplane can be observed:

Length-width ratio	Unfolded airplane	Upper view of the airplane	Side view of the airplane
1 : 0.45	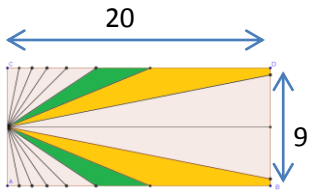		
1 : 0.75	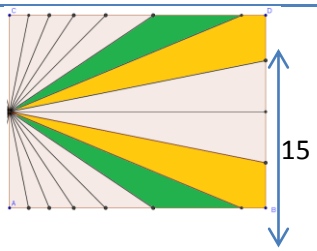	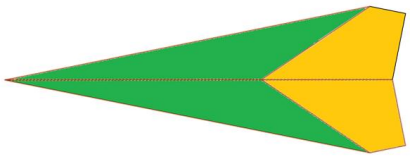	
1 : 0.95	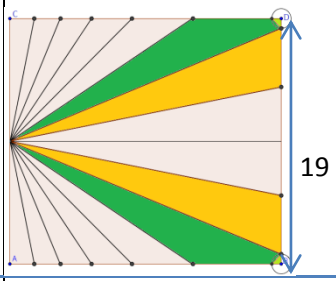	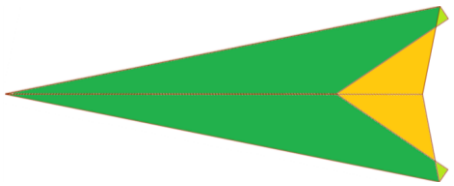	
1 : 1.1	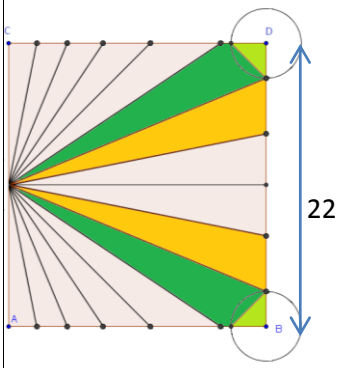	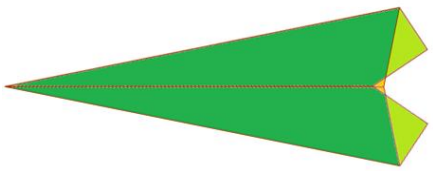	
1 : 1.35	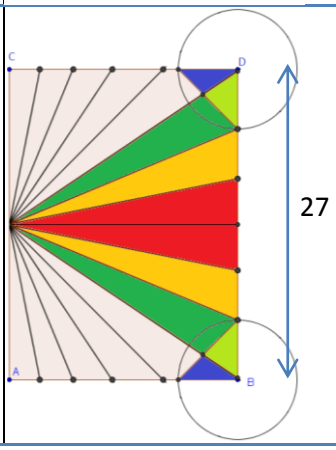	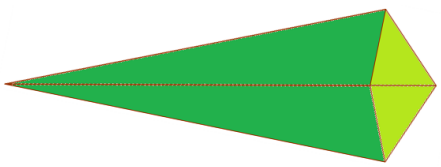	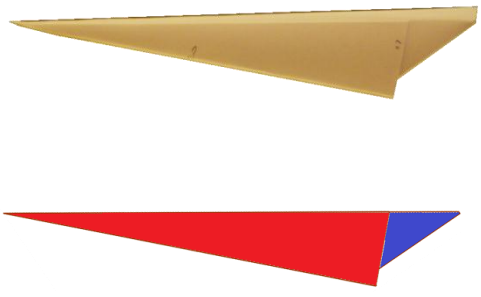

Table 1

As the width increased, the wingspan point was pushed back, until it reached the corners of the sheet (points B and D on the unfolded airplane diagram), to engender the formation of additional winglets – coloured light green – and of a "tail" (coloured blue) which emerged from the body of the airplane (coloured red). Complete convergence of the winglets occured at ratios bigger or equal to 1 : 1.3 (illustrations available in appendix A) .

One of the most noticeable changes was the increase in planform area, which continually increased as the width increased until the winglets converged completely. An increase in wingspan was also noted until it reached its maximum when the wingspan point reached the corners of the sheet.

Another transformation which has to be taken into account occured inside the airplane. The frontal parts of the wings of a folded dart are constituted of four layers of paper each, whereas that of the body is constituted of eight (see figure 5).

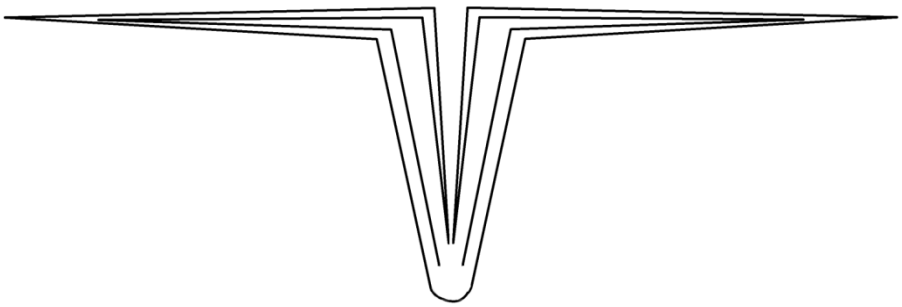

Figure 5 : Front view of a dart with a removed tip (not to scale)

Consider the unfolded paper airplane below: The four layers of the wing are the purple, light blue, green and orange areas on figure 6, which, when folded, superpose as shown in figure 7:

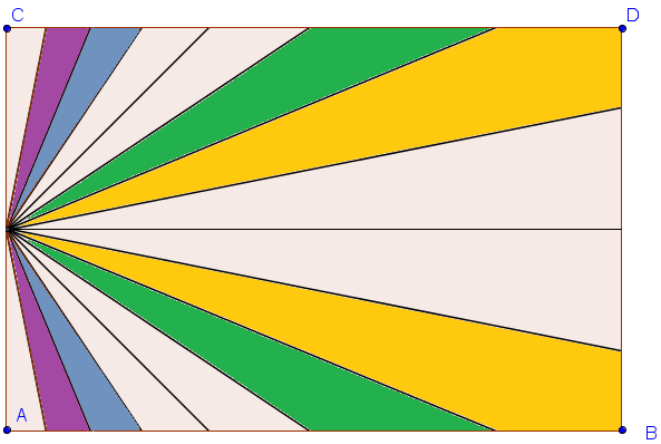

Figure 6 : unfolded airplane representation

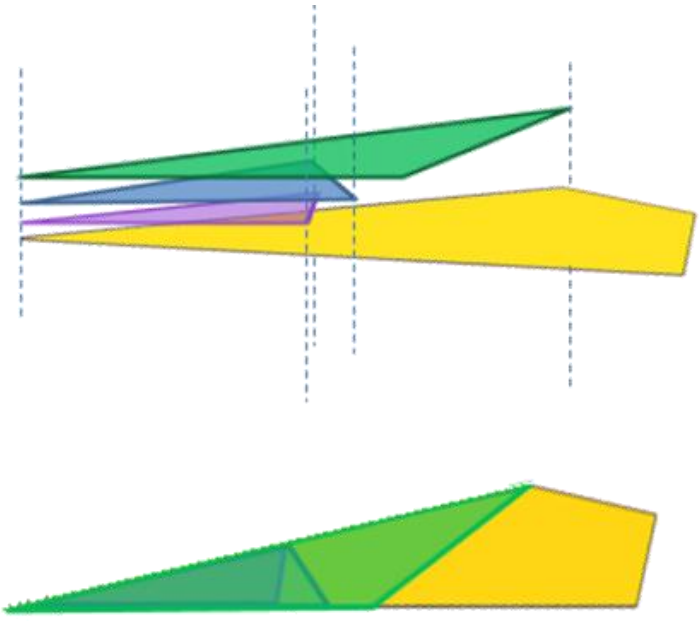

Figure 7 : Anatomy of a wing

However these areas, being proportional to the dimensions of the sheet of paper, elongate as the width increases, hence increasing the average thickness of the wing. This has for consequence to change the wing profile for every change in width, which therefore may have had an effect on the lift and drag properties of the airplane.
A very similar change occurs to the body, as its eight constituent layers also extend to increase the average thickness of the body, an increase which may have affected the drag coefficient of the dart.

Deriving the lift and drag coefficient and comparing the drag polar curves of darts made from different length-to-width ratios allows a better overview caused by the effects of the structural changes which occured, regardless of the changes in wing area and weight. However to determine which ratio produced the best airplane, both the efficiency of the airplanes and their overall (theoretical) ability to glide, which accounts for their ability to counteract their own weight, was also considered.

II: Method

To obtain a wide range of length-to-width ratios, twenty paper darts were built, all of which had a constant length of 20 cm, and a width varying from 9 cm to 29 cm at one centimetres intervals. The following folding procedure was used for all darts:

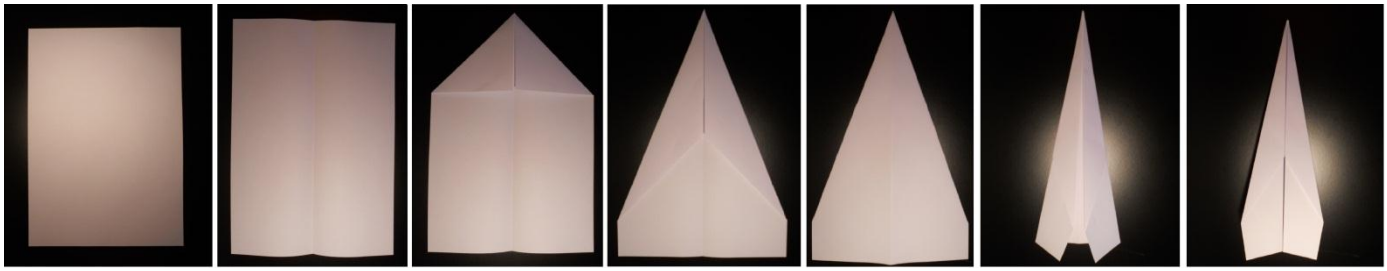

Figure 8: folding prodedure

The same type of paper (density of 120 g/m²) was used to construct all airplanes and the body and wings were stuck together at several points as similarly as possible using double-sided sticker tape to clearly define the variable of planform area, hence avoiding the effects of a centrefold and potential folding inaccuracies.

In order to graph the drag polar of the paper airplanes and hence determine their aerodynamic efficiency, it was necessary to find the lift and drag coefficients, which are defined by the following equations:

$$C_L = \frac{2 \times L}{\rho \times v^2 \times S}$$

$$C_D = \frac{2 \times D}{\rho \times v^2 \times S}$$

$C_L = Lift\ coefficient$
$C_D = Drag\ coefficient$
$L = Lift\ force$
$D = Drag\ force$
$\rho = Fluid\ density\ (air)$
$v = \ Relative\ velocity$
$S = Planform\ Area$

To calculate the Lift and Drag forces, all planes were subjected to wind tunnel testing at *the von Karman Institute for Fluid Dynamics*, in the SLWT-1 wind tunnel (more information available in appendix D) and each of the twenty planes was tested for lift and drag at angles of attack ranging from 0 to 50°, at 5° intervals.

The apparatus used to measure the Drag force (figure 9), was constituted of a 3 axis support system, which could pivot on the external structure to convert the horizontal drag force into a vertical force, which could then be measured by the 0.05 gram sensitive digital balance. The balance was calibrated to the weight of the apparatus (including the plane to avoid error), and the additional drag created by the vertical rod was subtracted from all results. After being recorded and corrected, the results were converted into Newtons.

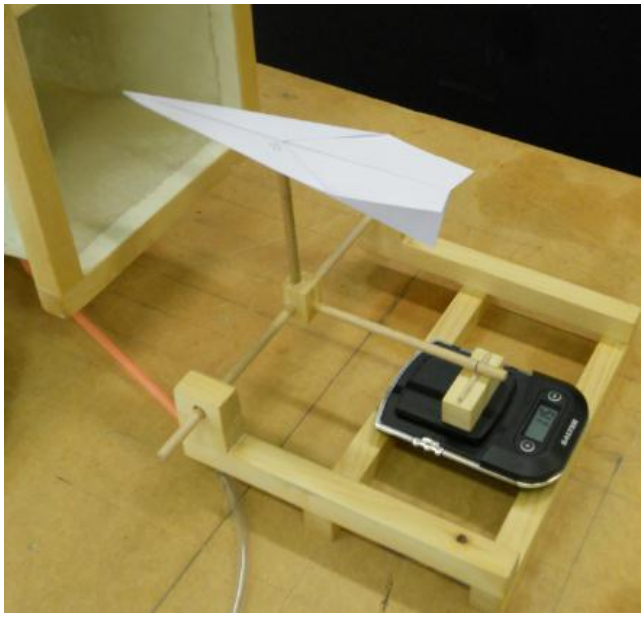

Figure 9 : drag measuring apparatus

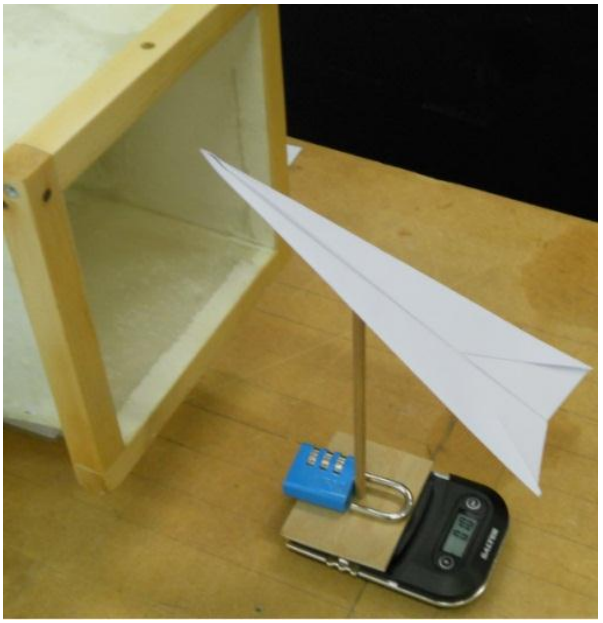

Figure 10 : lift measuring apparatus

The apparatus used to measure the Lift force, shown in figure 10, is constituted of a vertical wooden pole, a wooden support, counterweights and the same digital balance. The digital balance was calibrated to the weight of the entire apparatus, including the airplane, in order to measure the lift mass only (displayed as negative grams on the balance), and the modulus of the results were then converted into Newtons.

Ten paper squares of equal dimensions were marked by a straight line of reference which joined the midpoints of two opposite sides of the square. Each angle of attack investigated was then drawn on a square, with respect to the line of reference. The squares were then folded in order for them to fit the dart at the exact same position, the line of reference being the normal to the lower wing surface. The rod was then aligned to the angle line of the desired paper square to incline the darts at that very same angle of attack (figure 11).

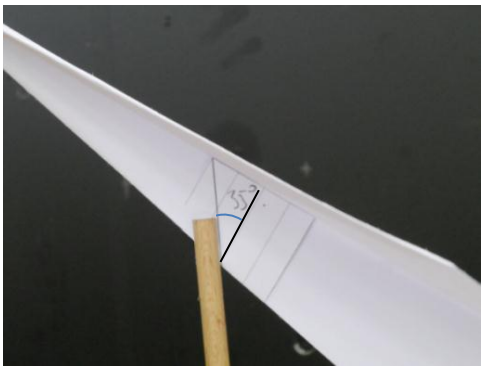

Figure 11

The planform area of each dart was calculated by drawing the unfolded airplane diagram on a geometry software, and using its area calculation application to find the area of the relevant zones - coloured yellow and light green in table 1 (introduction).

The velocity of the fluid was calculated using a U-tube manometer, connected to a straw, placed outside the wind tunnel opposite the flow of air.By measuring the difference in height *h* created by the pressure difference, and knowing the density of the liquid inside the tube (water) and the density of the air, the velocity of the fluid exiting the wind tunnel was found using the equation:

$$v = \sqrt{\frac{2\times \rho_w \times h \times g}{\rho_a}}$$

$v = velocity$
$\rho_w = \ density\ of\ water$
$\rho_a = density\ of\ air$
$h = difference\ in\ height$
$g = gravity$

The manometer was inclined on a 20% gradient slope to amplify the difference in height, which was 9.25 centimetres. The real value of h was therefore a fifth of this value, hence the recorded value of *h* for the experiment being 0.0185 metres. The density values used for water and air were 1000 kg/m³ and 1.2250 kg/m³ respectively [4] [5]. The calculated value of fluid velocity was therefore 7.8 m s^{-1} (calculation available in appendix C).

Although it is the *ratio* of length to width which is being investigated, specific paper darts were referred to by their respective width value, throughout parts of this investigation for ease in data interpretation (e.g. the paper dart of format 16×20 will be referred to as dart number 16).

III. Results and Analysis

The processed data was arranged in the form of the drag polar curve of each individual dart. However, the variations in efficiency of the darts can be compared more easily by plotting the graph of lift coefficient-to-drag coefficient against their respective dart number at different angles of attack (all the individual drag polar curves can be found in appendix B).

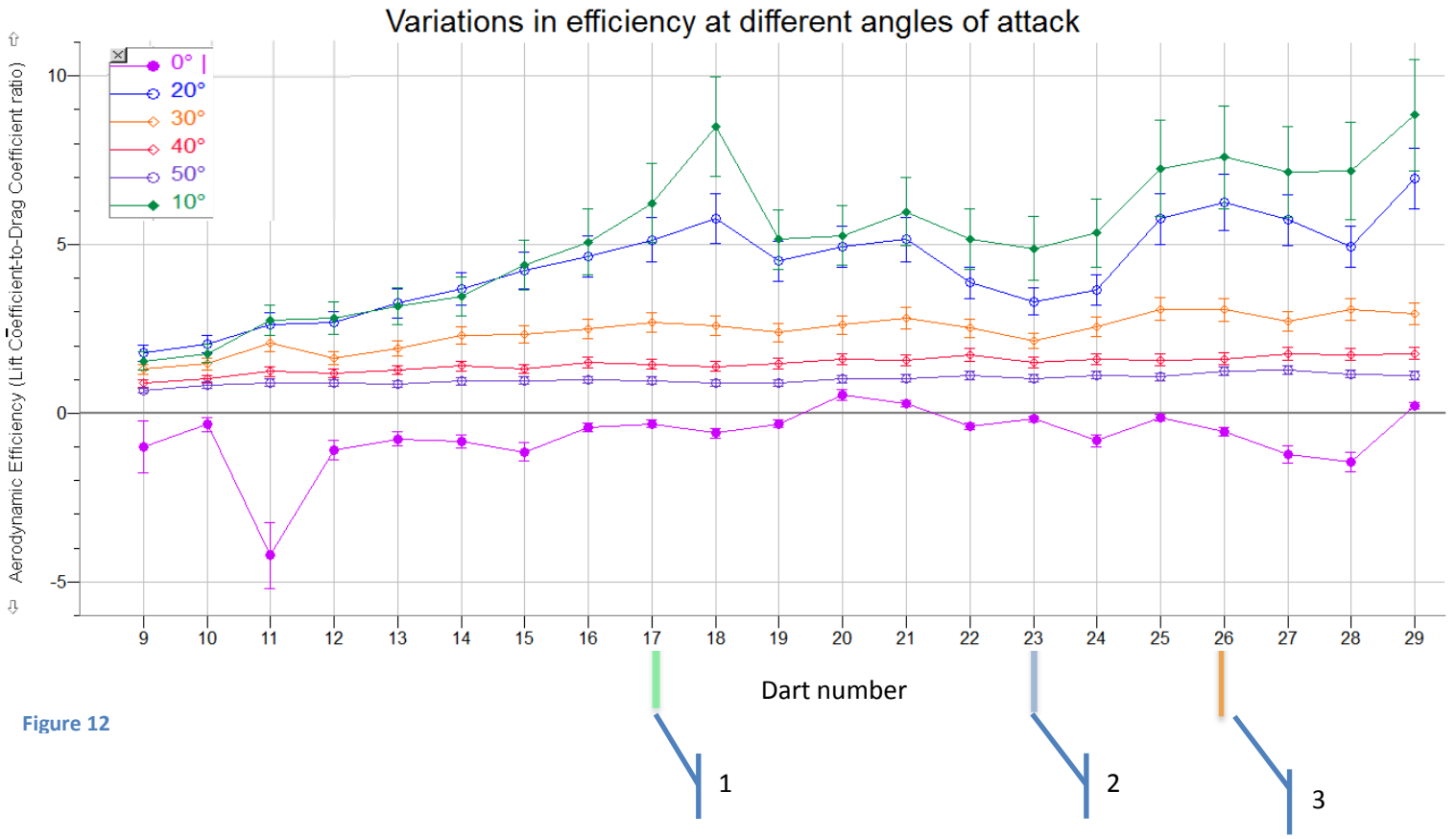

Figure 12

The general pattern observed saw a regular increase can be seen in the values of the first 9 planes, before dropping greatly for plane number 19. A second rise was seen for planes 20 and 21, before dropping again, to reach a minimum at plane number 23. A third rise was recorded from planes 24 onwards peaking at 26, before descending a last time, finding its turning point at plane 28, to rise a final time for plane number 29 (the graph displaying the data for all angles of attack can be found in Appendix B).

The vertical coloured lines on the graph indicate the most noticeable changes occurring on the paper airplane's design:

Line number 1 (green) marks the point at which additional winglets start to form at the back of the airplane.

Line number 2 (blue) marks the starting convergence of the winglets and the start of the development of the tail.

Line number 3 (orange) marks the completed convergence of the winglets. (illustrations available in appendix A)

The data presented in figure 12 indicates that planes number 18, 21, 26 and 29 had some of the highest lift coefficient-to- drag coefficient ratio at angles of attack ranging from 0° to 40°, and were therefore the most aerodynamically efficient designs.

Having found the aerodynamic efficiencies of each specific structure, their ability to glide was also investigated in order to determine the most suitable ratio overall, and then create the best paper dart possible. The ability of a dart to glide depends on how well it counteract its own weight with the lift force it generates. Substracting the weight of a dart from the lift it generates results in what can be called the net lift force:

$$Airplane\ weight = Area\ of\ constituent\ paper\ sheet \times paper\ density \times gravity$$
$$Net\ lift\ force = Lift\ force - airplane\ weight$$

Seeing as, for a dart to glide as well as possible, it must have the highest net lift force while keeping the lowest drag lift force as possible, the ability to glide can be defined as the ratio of net lift force-to-drag force. Therefore, plotting the net lift force of each dart against its respective drag force at different angles of attacks allowed this ratio to be displayed visually (gradient between the origin and the desired point):

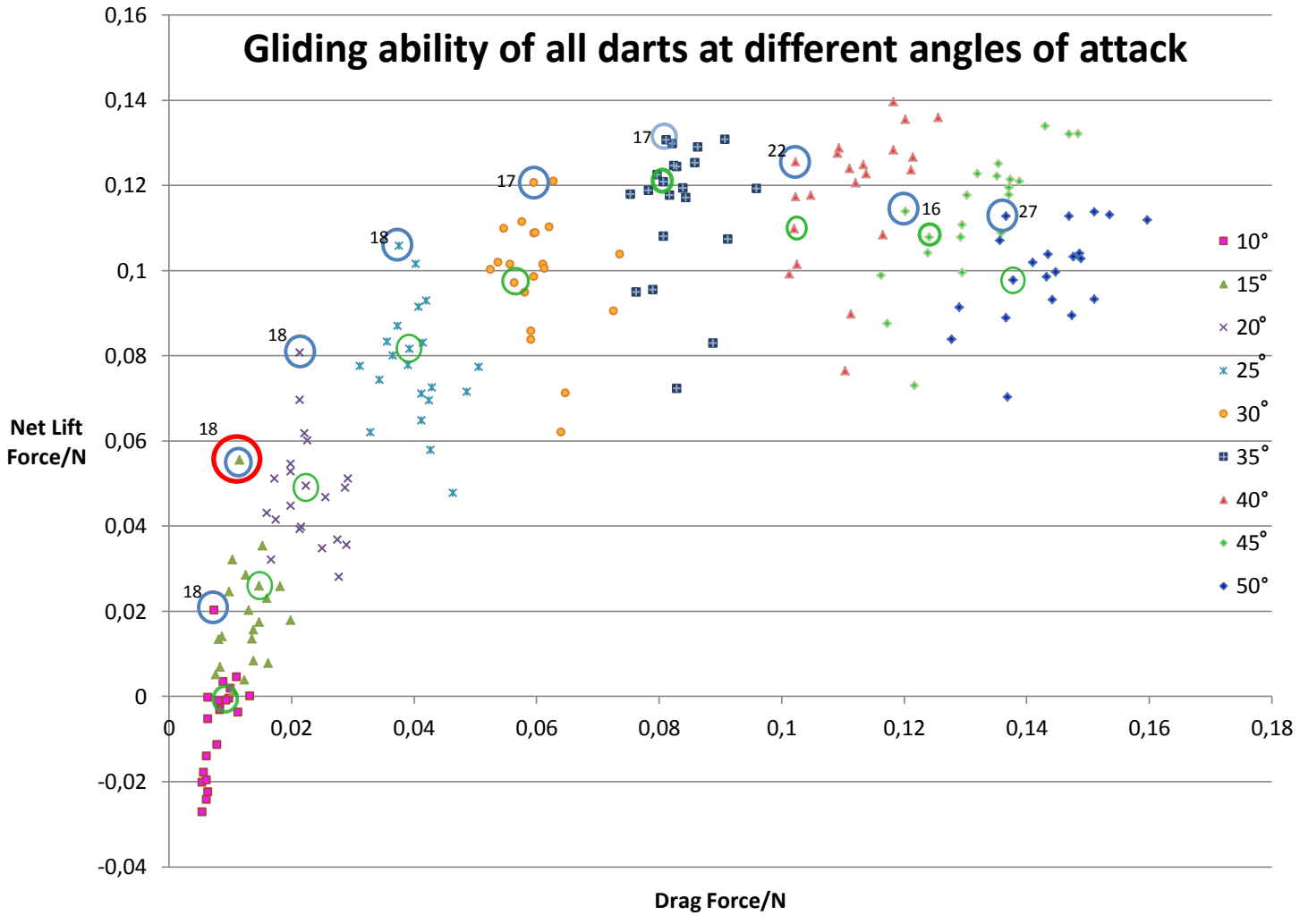

Figure 13

Graphing the data using the following method allowed the dart with the highest net lift force-to-drag force ratio (circled in blue) to be found easily for each angle of attack. Additionally, it also indicated clearly the optimal angle of attack - dart combination, the combination of the dart and the angle of attack which resulted in the highest overall ratio (circled in red). The values circled in green refer to paper dart number 14, which has a length-to-width ratio of 1 : 0.7, similar to that of an A4 sheet of paper.

The highest net lift force-to-drag force ratio was achieved by dart number 18, for angles 10°, 15°, 20° and 25°and dart number 17 achieved the highest ratio for angles 30° and 35°. Angles 0° and 5° were not plotted on the graph as all values for net lift of attack – dart combination was achieved by dart number 18, at an angle of 15°.

VI. Conclusion and Explanatory Theories

Comparing the efficiency and the gliding ability data sets, plane number 18 seems to be the superior design: It's aerodynamic efficiency was amongst the highest at force were negative, meaning none of the darts could fully counteract their weight at those angles. The optimal angle

angles 10°, 15°, 20° and 25°, and was above average for angles 0°, 5°, 30°. Its gliding ability was the highest for angles 10°, 20° and 25° and 15°, which was the optimal combination. Seeing as paper darts are usually thrown at an angle ranging from 0° to 40°, this shows that dart number 18 is the best model.
Paper dart number 14, on the other hand, had relatively low values of aerodynamic efficiency and average values of gliding ability. It can therefore be concluded that the sheet 18 centimetres wide and 20 centimetres long, not the classic A4 format, produced the most efficient airplane, and that the most adequate length to width ratio of a paper sheet to be used to create the most efficient paper dart product is therefore $1:0.9$

I believe the data collected during this investigation, in addition to supplementary background knowledge, points towards the following possible explanations for the interesting behaviour the paper darts showed throughout my research. However, these remain theories and have no other support than the arguments presented in this section.

Looking back at the aerodynamic efficiency data plot (figure 12), the fluctuations in efficiency are likely to be the result of the structural variations of the paper dart model, such as the additional winglets and increased wing and body thickness, as the efficiency was dependent on neither the wing area nor the plane's weight.

The regular increase in aerodynamic efficieny which occurred from dart number 9 till dart number 18 may only have been caused by a change in wing profile, as the only structural variation which took place for this range of width values were internal changes. However, the sudden drop in efficiency for dart number 19 coincided with the fomation of winglets. Although dart number 18 was the first to show the formation of winglets, they were very small and were probably insignificant, which may be the reason why dart number 18 did not lose any aerodynamical efficiency like dart 19 did. This implies that these winglets may have been the cause of a change of airflow over the dart:

Vortice Theory:

The difference in pressure between the superior and inferior layers of the wing causes air from the high pressure zone under the wing to curve around the leading edges of the wing to reach the low pressure zone above the wing, as shown in figure 14, and causing turbulent flow called vortices, which results in an increase in drag.

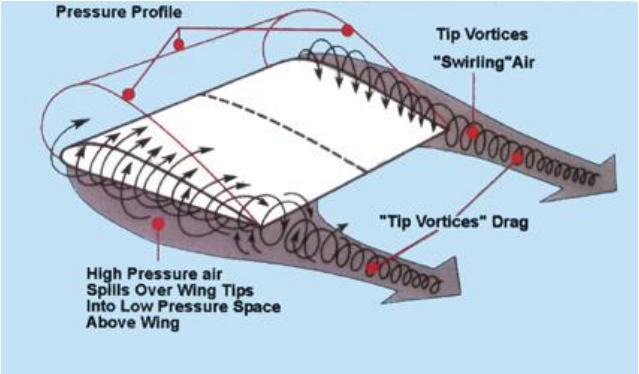

Figure 14 : Vortices of a standard wing

It was therefore probable that the formation of winglets altered the formation of the vortices, consequently also altering the drag coefficient.

Consider airplane number 17 (figure 15). The nearly perfect delta planform results in two vortices at each wingtip, causing relatively little drag. However, the appearance of winglets may have caused additional vortices to be created, as seen on plane number 23 (figure 16).

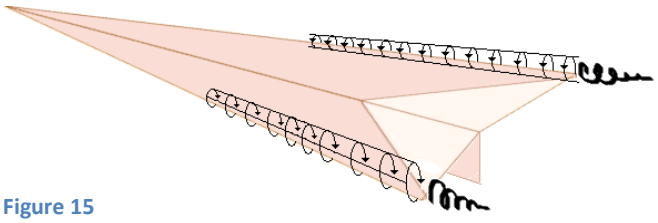

Figure 15

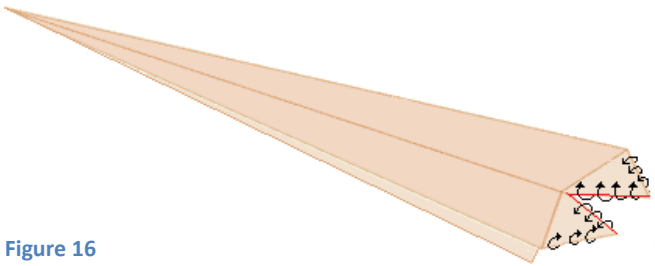

Figure 16

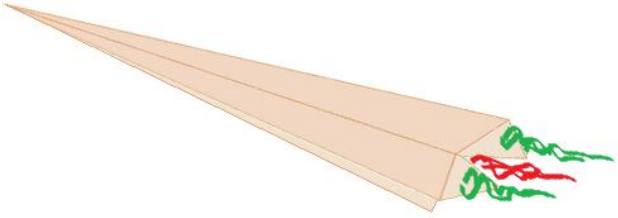

Figure 17

The opposing flows of air currents around the winglets could have caused a zone of turbulence (in green on figure 17), both on the winglet and behind it, causing the airplane to endure additional drag. The vortices caused by the inner edges of both winglets (coloured red on figure 16) are also likely to have interfered with each other to create an additional zone of turbulence – the "intermediate" zone of turbulence (coloured red on figure 17).
This theory is supported by the data presented in figure 12: The lift coefficient to drag coefficient ratio started to decrease as the winglets started to have a significant size which made the generation of turbulences around them possible. The ratio values decreased to find a minimum with plane number 23, which corresponds to the point where the winglets started converging (see appendix A), meaning they were large enough to generate more important turbulence zones, and close enough together for these turbulence zones to interfere together and create the intermediate interference zone. As the width increased further, the gap between the winglets gradually narrowed accordingly which allowed less air to arise from under the winglets through the central gap. This led to the gradual merging of the two zones of turbulences, and the disappearance of the intermediate interference zone of turbulence. As these changes occurred, the lift coefficient-to-drag coefficient ratio started to rise again accordingly until the complete convergence of the winglets (which occurred from plane 26 onwards).

V. Practical application

Although the data showed that airplane number 18 was the most efficient paper dart model, additional factors need to be considered before concluding that it will be the best glider when tested in practical: The most important factor which will affect the flight path of the dart and which was not taken into account in this investigation is the position of the centre of gravity in relation to the centre of lift of the plane.

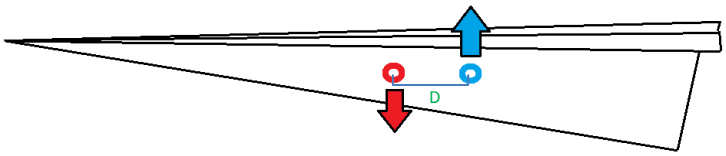

Figure 18

The position of the centre of lift (in blue on figure 18), which acts as the pivot, in relation to the position of the centre of mass (in red on figure 18) will determine the overall horizontal torque of the dart, which is calculated by the following formula [6]:

$$T = D \times F$$

$T = torque$
$D = distance\ between\ the\ force\ and\ the\ pivot$
$F = Force$

In the case when the centre of gravity is positioned in front of the centre of lift, the tip of the dart will sink, causing the airplane to lose altitude. However, in the case when the centre of gravity is positioned behind the centre of lift, the tip will rise, causing the airplane to lose velocity, gain altitude, and increase its angle of attack until it reaches the stalling point which could lead to a crash (figure 19). The rate of change in altitude will be proportional to the resultant torque and therefore proportional to the distance between the centre of lift and the centre of drag. To obtain a stable flight and hence maximize the flight duration and distance, the centre of gravity should be placed in front of the centre of lift, close as possible to it, the optimum point being the overlap of the two points as no resultant torque would be produced, unaffected by the angle of attack.

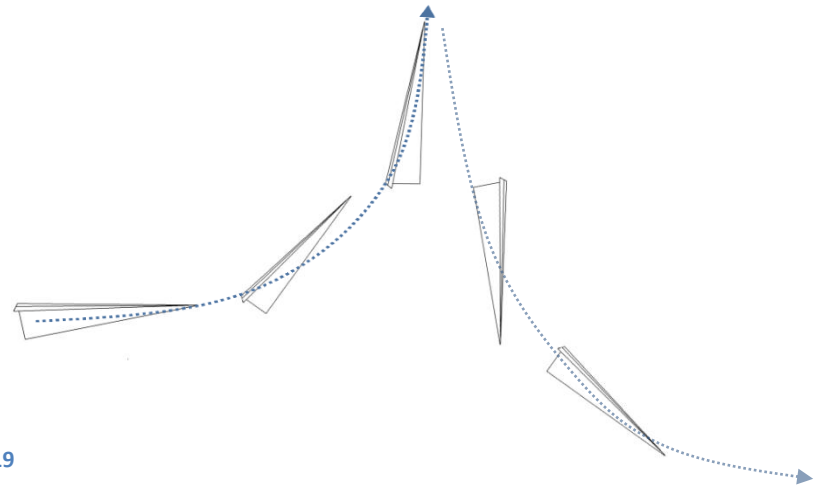

Figure 19

It is likely that their relative position will evolve as an additional consequence of varying paper sheet ratio, and the position of the centre of lift and centre of gravity must therefore be taken into account before acknowledging the gliding ability of plane number 18 as being the best.

VI. Evaluation

The results on which the conclusion of this Extended Essay is based were the consequences of the combination of different factors, such as the formation of winglets, a tail and changes in body and wing thickness. The individual, isolated effects of these variables were quite difficult to conclude, and further investigations would be necessary to determine for certain their contribution to the changes in the aerodynamic properties of the different airplanes. Suggestions of follow up investigations include:

1. Repeating the experiment, but removing the additional winglets and tail in order to investigate the effect of changing wing and body thickness.
2. Repeating the experiment using a single airplane model, but adding winglets of different sizes, investigating their effect by keeping the same length to width ratio.
3. Conduct airflow tests on all original airplanes to verify the theory put forward in the results section regarding the behaviour of the darts' vortices and their effect on the drag coefficient of the the airplanes.

Appendix A

Formation of winglets:

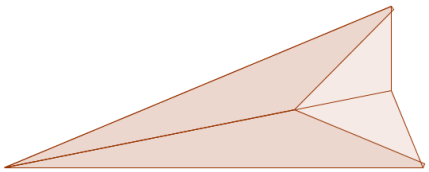

Dart number 17 (ratio 1 : 0.85): Start of the formation of winglets

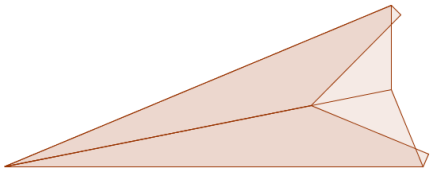

Dart number 18 (ratio 1 : 0.90)

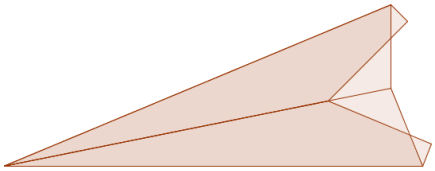

Dart number 19 (ratio 1: 0.95)

Convergence of winglets:

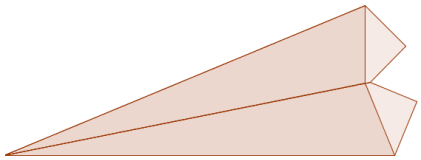

Dart number 23 (ratio 1 : 1.15): Start of the convergence of winglets

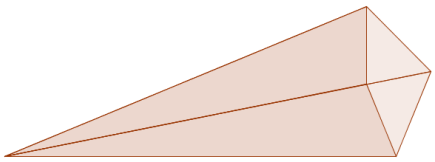

Dart number 26 (ratio 1 : 1.3): complete convergence of winglets

Appendix B

The collected data below is presented in the form of the drag polar curve of the darts, and displayed in groups of 3 data sets for clarity and ease of comparison.

Drag polar curves of airplanes # 9, 10 and 11

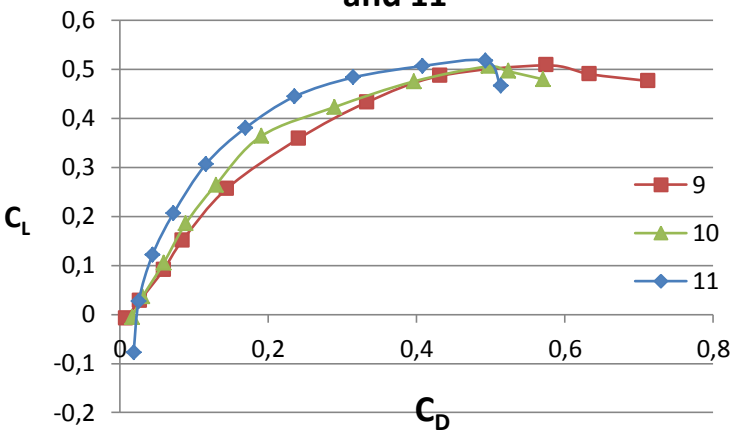

Drag polar curves of airplanes # 11, 12 and 13

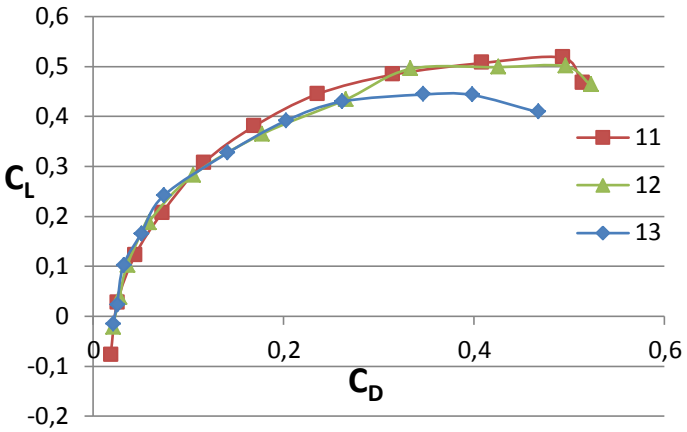

Drag polar curves of airplanes # 13, 14 and 15

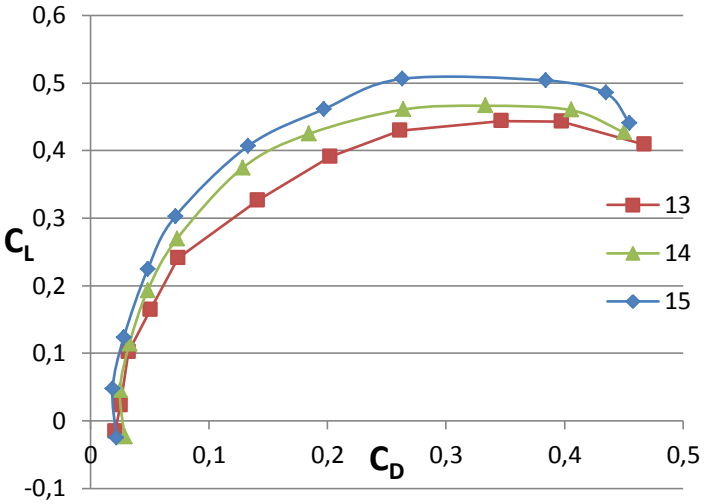

Drag polar curves of airplanes # 15, 16 and 17

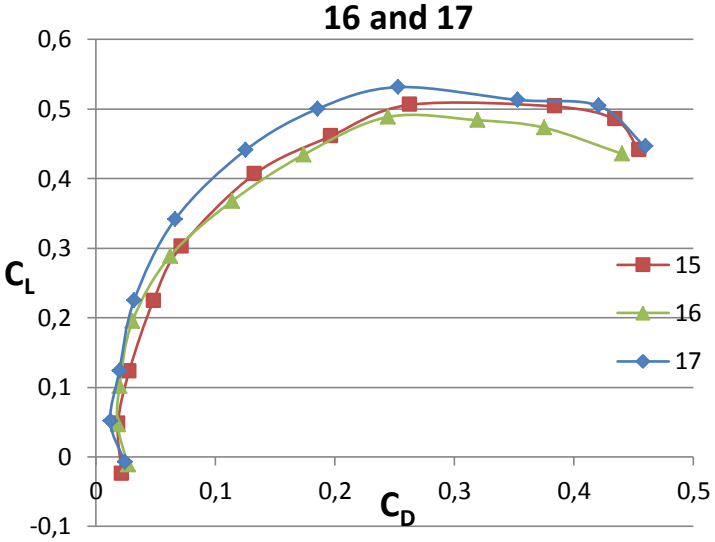

Drag polar curves of airplanes # 17, 18 and 19

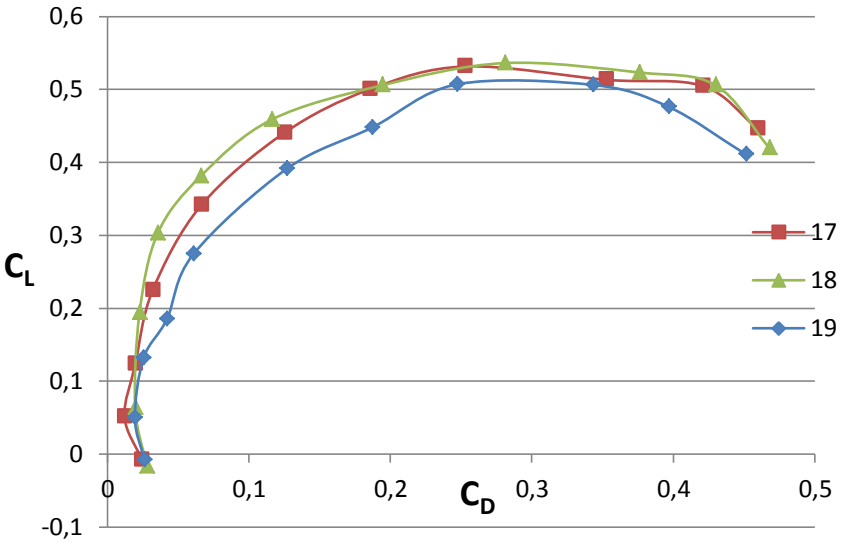

Drag polar curve of airplanes #19, 20 and 21

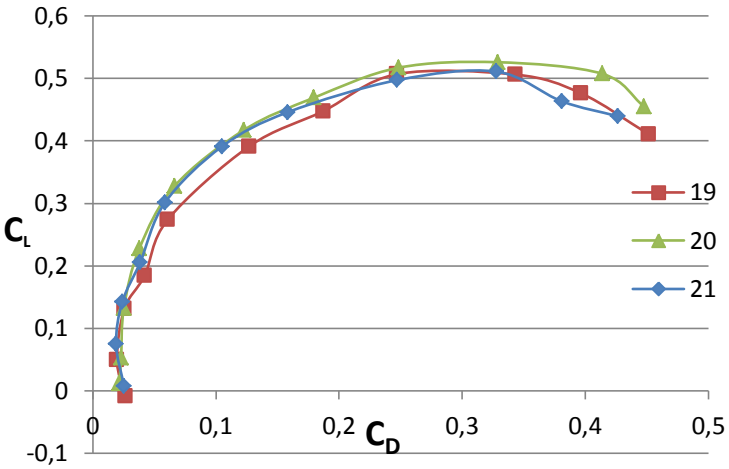

Drag polar curves of airplanes # 21, 22 and 23

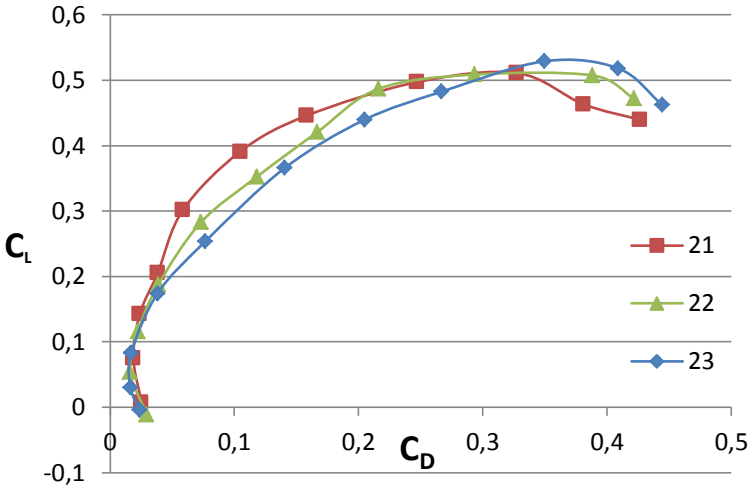

Drag polar curves of airplanes # 23, 24 and 25

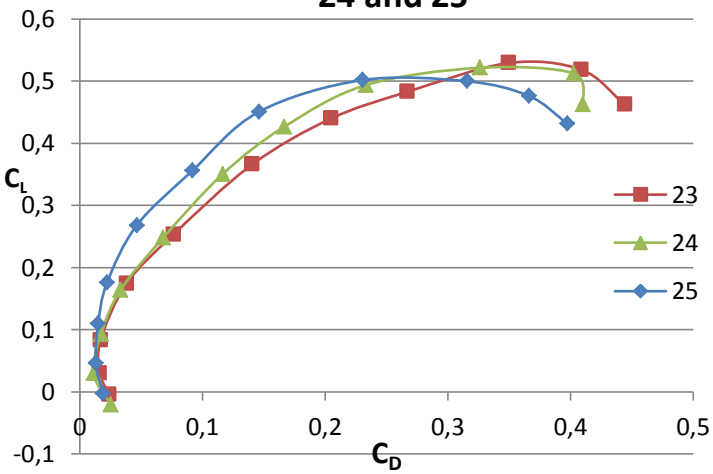

Drag polar curves of airplanes # 25, 26 and 27

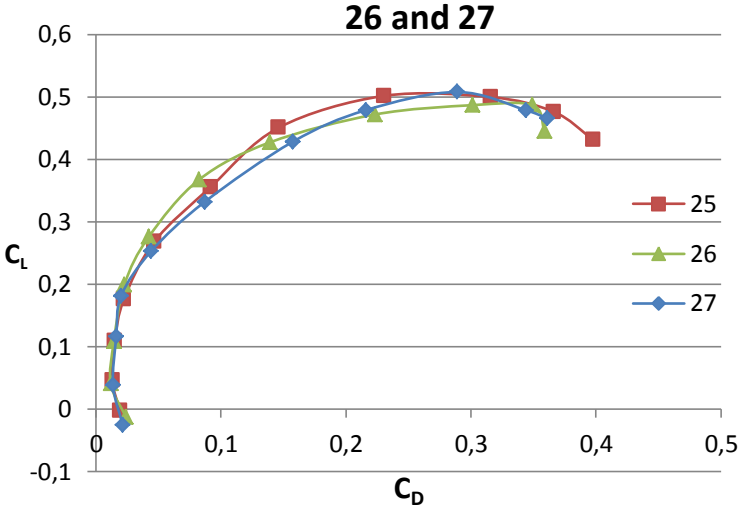

Drag polar curves of Airplanes # 27, 28 and 29

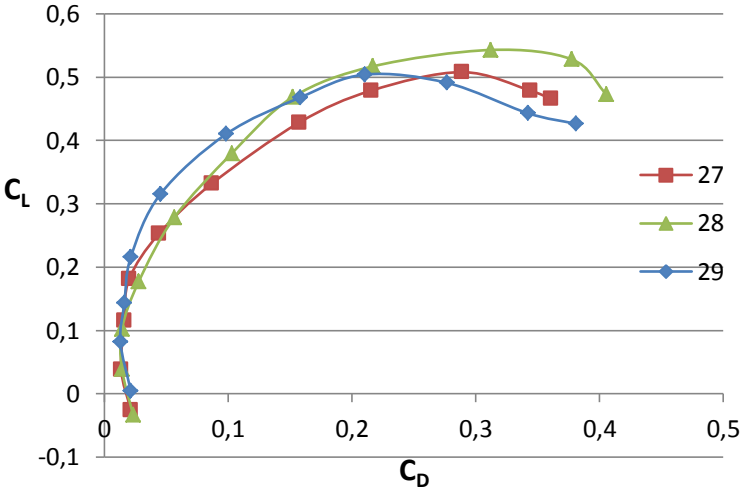

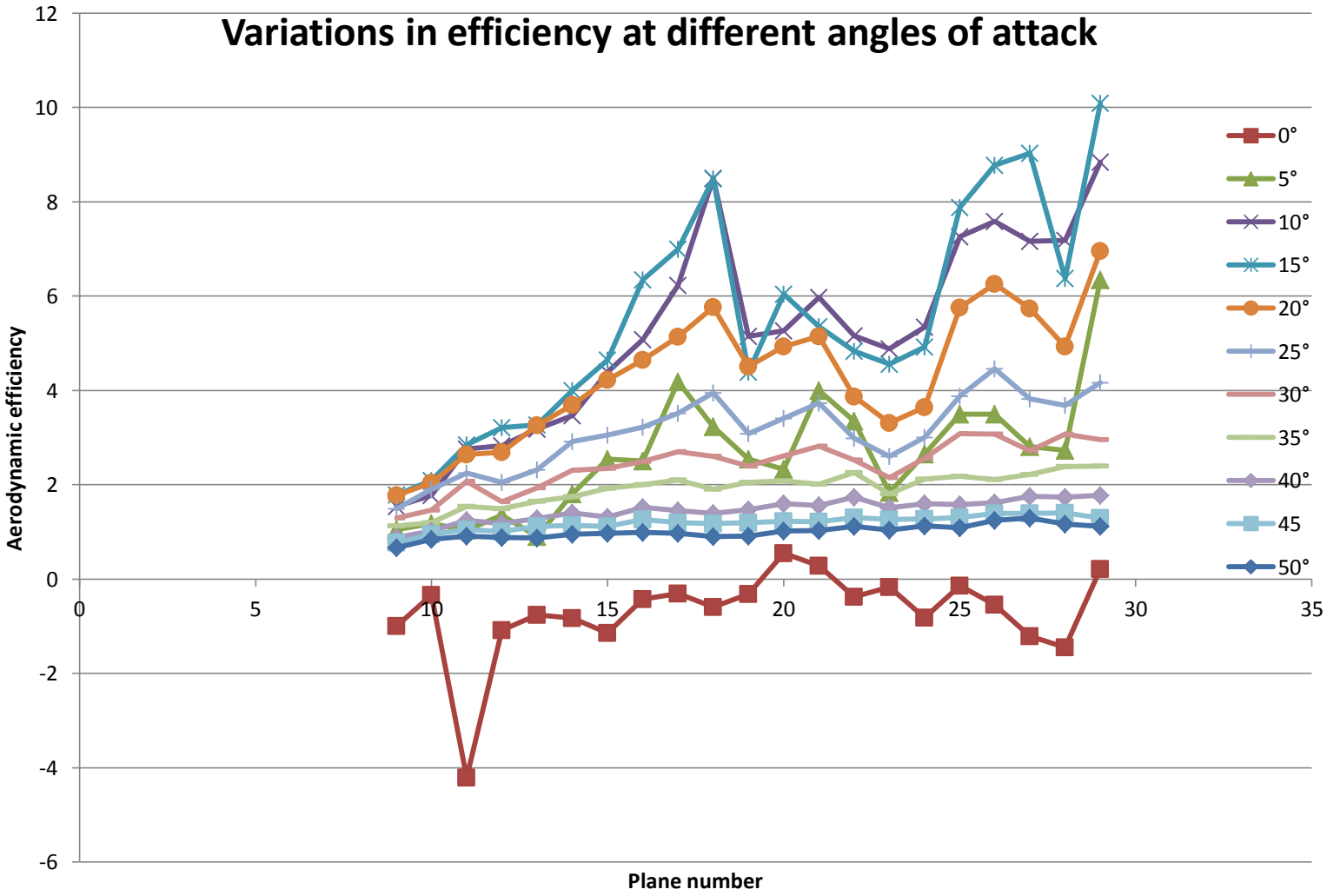
Variations in efficiency at different angles of attack
Aerodynamic efficiency
Plane number
12
10
8
6
4
2
0
-2
-4
-6
0
5
10
15
20
25
30
35
0°
5°
10°
15°
20°
25°
30°
35°
40°
45
50°

Appendix C

Uncertainties:

The uncertainties for all planes were calculated using spreadsheets. Below is an example of the calculations followed to obtain the uncertainties in length, surface area, fluid velocity, lift and drag forces, lift and drag coefficients and aerodynamic efficiency. The example refers to plane number 9 at an angle of attack of 0°:

Uncertainty in width and in length: $\pm 0.05\ cm$ (as the ruler used to measure was divided in millimetres)

$$Percentage\ (\%)\ uncertainty\ in\ surface\ area = \%\ uncertainty\ in\ length + \%\ uncertainty\ in\ width$$

$$\boldsymbol{Therefore, \%\ uncertainty\ in\ surface\ area} = \frac{0.05}{20} \times 100 + \frac{0.05}{width\ (9)} \times 100\ = 0.806\ \%$$

Uncertainty in (fluid velocity)²: $\%\ uncertainty\ of\ inclined\ h\ +\ \%\ uncertainty\ in\ gradient$

$$\%\ uncertainty\ of\ inclined\ h = \frac{0.05}{9.25} \times 100 = \pm 0.541\%$$

$$\%\ uncertainty\ in\ gradient = \%\ uncertainty\ of\ \Delta x\ \left(\frac{0.05}{9} \times 100\right) +\ \%\ uncertainty\ of\ \Delta y\ \left(\frac{0.05}{1.8} \times 100\right) = 3.33\%$$

Hence, $\%\ Uncertainty\ of\ h = 0.541\ + 3.33 =\ \pm 3.87\%$

As the values for water density, air density and gravity were obtained from another source, their uncertainty was not found and it was therefore assumed that it was negligible.
$The\ uncertainty\ in\ fluid\ velocity^2\ is\ therefore\ \pm 3.87\%$

Uncertainty in lift force: $\pm\ 0.05\ grams,\ hence\ \pm 0.0004905\ Newtons.$

$$Hence, \%\ uncertainty\ in\ lift\ force = \left|\frac{0.0004905}{Lift\ force\ value\ (-0.0014715)}\right| \times 100 = \pm 33.3\%$$

% Uncertainty in lift coefficient:
$\%\ uncertainty\ of\ surface\ area +\ \%\ uncertainty\ of\ velocity^2 +\ \%\ uncertainty\ of\ lift\ force$
$= 0.806 + 3.87 + 33.3 = 37.976 = 38\%$ (3 s.f.)

In order to calculate the Uncertainty in drag coefficient, the same procedure was followed as for the lift coefficient, with for only variable the % uncertainty in drag force:

$$Hence, \%\ uncertainty\ in\ drag\ force = \frac{0.0004905}{drag\ force\ value\ (0.0014715)} \times 100 = \pm 33.3\%$$

% Uncertainty in drag coefficient:

$\%\ uncertainty\ of\ surface\ area + \%\ uncertainty\ of\ velocity^2 + \%\ uncertainty\ of\ lift\ force$
$= 0.806 + 3.87 + 33.3 = 37.976 = \pm 38\%$ (3 s.f.)

% Uncertainty in efficiency = $\%\ uncertainty\ of\ lift\ coefficient + \%\ uncertainty\ of\ drag\ coefficient$
$= 38 + 38 = \pm 76\%$

Airspeed calculations:

$$\boldsymbol{v} = \sqrt{\frac{2 \times\ 1000\ \times 0.0038\ \times 9.81}{1.22521}}$$

$$= \sqrt{60.85}$$

$$= 7.8\ \text{m s}^{-1}$$

Appendix D

Wind tunnel used in the investigation:

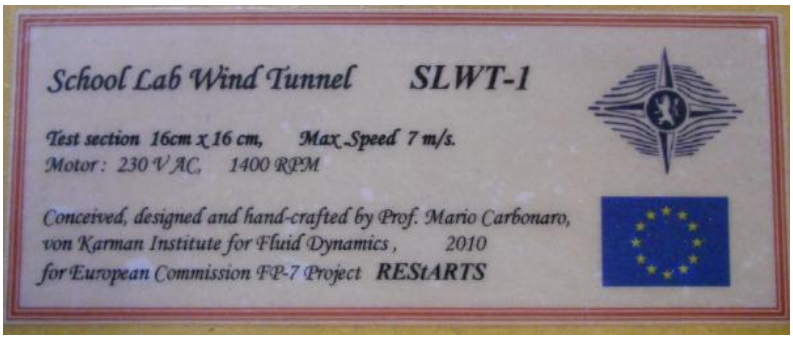

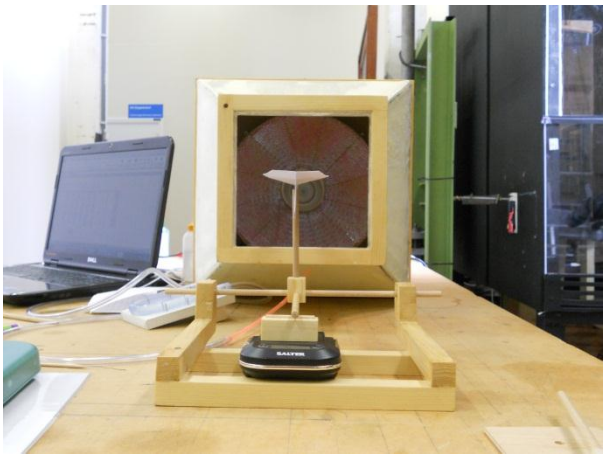

"VKI is a non-profit international educational and scientific organisation, hosting three departments (aeronautics and aerospace, environmental and applied fluid dynamics, and turbomachinery & propulsion). It provides post-graduate education in fluid dynamics **(research master in fluid dynamics, former "VKI Diploma Course", doctoral program, stagiaire program and lecture series**) and encourages "training in research through research". The von Karman Institute undertakes and promotes research in the field of fluid dynamics. It possesses about fifty different wind tunnels, turbomachinery and other specialized test facilities, some of which are unique or the largest in the world. Extensive research on experimental, computational and theoretical aspects of gas and liquid flows is carried out at the VKI under the direction of the faculty and research engineers, sponsored mainly by governmental and international agencies as well as industries." - https://www.vki.ac.be/index.php?option=com_content&view=category&layout=blog&id=73&Itemid=371

The *Von Karman Institute for Fluid Dynamics* official website: http://www.vki.ac.be/

List of Figures:

References

Literature:

- Encyclopædia Universalis, Dictionaire de la Physique mécanique et thermodynamique, Albin Michel 2001, "AÉRODYNAMIQUE", pp 55-61
- R. Halleux, Sabena Training Department, Performance refresher course for Instructors, 1987, section 1 pp 16.

Softwares:

- Geogebra 4 – http://www.geogebra.org/cms/en/download

World Wide Web resources:

- http://www.paperplane.org/Aerodynamics/paero.htm (Accessed February 18th, 2011)
- http://hyperphysics.phy-astr.gsu.edu/hbase/pber.html#beq (Accessed March 1st, 2011)
- [1]: Ng Bing Feng, Kng Qiao Mei, Pey Yin Yin and Jörg U. Schlüter, "On the Aerodynamics of Paper Airplanes", Nanyang Technological University, School of Mechanical and Aerospace Engineering, Singapore URL: http://www.ntu.edu.sg/home/schluter/pdf/aiaa-2009-3958.pdf (Accessed February 18th, 2011)
- [2]: http://www.grc.nasa.gov/WWW/k-12/airplane/size.html (Accessed March 3rd, 2011)
- [3]: http://www.pilotsweb.com/principle/liftdrag.htm (Accessed July 13th, 2011)
- [4]: http://en.wikipedia.org/wiki/Density_of_air (Accessed February 18th, 2011)
- [5] http://en.wikipedia.org/wiki/Properties_of_water#Density_of_water_and_ice (Accessed December 11th, 2011)
- [6] http://www.grc.nasa.gov/WWW/k-12/airplane/torque.html (Accessed August 3rd, 2011)

Institutions:

- The Von Karman Institute for Fluid Dynamics, August 12th and August 16th, 2011.

Acknowledgements

I would like to thank Professor Mario Carbonaro and Professor Jeroen Van Beeck of the *von Karman Institute for Fluid Dynamics* for receiving me and advising me during my time spent at their institution.

I would also like to thank Mr François Gernaey for his greatly valued support, encouragements and for inspiring me.